CONF-860722--6

DESIGN RULE FOR FATIGUE OF WELDED JOINTS IN ELEVATED-TEMPERATURE NUCLEAR COMPONENTS[1]

D. G. O'Connor
J. M. Corum

Oak Ridge National Laboratory
Oak Ridge, Tennessee 37831

MASTER

CONF-860722--6

DE86 007569

ABSTRACT

Elevated-temperature weldment fatigue failures have occurred in several operating liquid-metal reactor plants. Yet, ASME Code Case N-47, which governs the design of such plants in the United States, does not currently address the reduced fatigue strength of weldments. To verify this shortcoming the Code Subgroup on Elevated Temperature Design recently proposed a fatigue strength reduction factor for austenitic and ferritic steel weldments. The factor is based on a variety of weld metal and weldment fatigue data generated in the United States, Europe, and Japan. This paper describes the factor and its bases, and it presents the results of confirmatory fatigue tests conducted at Oak Ridge National Laboratory on 316 stainless steel tubes with axial and circumferential welds of 16-8-2 filler metal. These test results confirm the suitability of the design factor, and they support the premise that the metallurgical notch effect produced by yield strength variations across a weldment is largely responsible for the observed elevated-temperature fatigue strength reduction.

INTRODUCTION

Construction of elevated-temperature Class 1 nuclear components is governed by ASME Boiler and Pressure Vessel Code Case N-47 (1). Currently that Case contains only minimal weldment design guidance that is based on actual weldment properties. However, that will change under recent Code Case N-47 modifications and additions approved by the Code Subgroup on Elevated Temperature Design and currently being considered by the Subcommittee on Nuclear Power (Section III). Under the modifications and additions, the allowable primary stress limits would be adjusted, where appropriate, to account for the frequently reduced creep-rupture strength of weld metal

---

[1]Research sponsored by the Office of Technical Support Programs, U.S. Department of Energy, under contract DE-AC05-84OR21400 with Martin Marietta Energy Systems, Inc.

DISTRIBUTION OF THIS DOCUMENT IS UNLIMITED

By acceptance of this article, the publisher or recipient acknowledges the U.S. Government's right to retain a non-exclusive, royalty-free license in and to any copyright covering the article.

relative to that of unaffected base metal. The creep-rupture portion of the creep-fatigue damage evaluation in Appendix T of N-47 would be similarly adjusted at weldments. Finally, a weldment fatigue strength reduction factor would be introduced to account for the strain concentration, and consequent fatigue life reduction, that can occur at weldments. This paper focuses on the proposed fatigue strength reduction factor. The factor and its bases will be described, and results from a small confirmatory test program, being undertaken at Oak Ridge National Laboratory (ORNL) on 316 stainless steel tubular specimens welded with 16-8-2 filler metal, will be presented.

The importance of addressing weldment fatigue in elevated-temperature reactor components, particularly liquid metal components, is emphasized by plant experience. Thermal fatigue has led to weldment cracking in a number of instances. For example, the French Phenix liquid-metal fast breeder reactor (LMFBR), while extremely successful overall, was initially plagued with several problems of weldment cracking (2,3). These included cracking at welds joining piping tees and valves to piping runs and cracking in intermediate heat exchanger welds. In each case the cause was identified as fatigue or creep-fatigue due to the repeated thermal transient loadings. It has been stated that these problems "cost the power station many months of unavailability, and constituted a considerable loss of earning power" (3). A second example is the British Dounreay Fast Reactor (DFR), which developed a leak in a primary circuit pipe weld (4). The stated cause was fatigue, and, again, the reactor had to be shut down for repairs. As a final example, Russian LMFBRs have reportedly also experienced weldment failures.

Although lessons regarding such things as weld placement were learned from these incidences, the need for explicit, experimentally based, design rules is clear. The Nuclear Regulatory Commission (NRC) recognized this deficiency during the licensing review of the Clinch River Breeder Reactor Plant for a construction permit (5). Early weldment cracking, particularly in components subjected to repeated thermal transient loadings, was identified by NRC as the foremost structural integrity concern, and a confirmatory test program was to have been required to determine the safety margins of weldments in elevated-temperature components (6).

In addition to residual stress effects, which are thought to be minimal at elevated temperatures, there are three possible primary contributors to early fatigue failure of weldments: (1) geometric discontinuities,

(2) inclusions and voids, and (3) metallurgical discontinuities. Class 1 nuclear welds are often ground flush; if they are not, Code Case N-47 requires that the actual weld geometry be taken into account in design analyses. Thus, the geometric discontinuity problem is accounted for already. Inclusions and voids are not expected to play a significant role. A recent Japanese paper (7) showed that, unlike room-temperature results, elevated-temperature fatigue strength is not significantly affected by weld defects, at least for the austenitic weldment that was studied. Furthermore, since Class 1 nuclear weldments are subjected to rigorous inspection procedures, the possibility of a weldment containing significant voids or inclusions is minimal. This leaves metallurgical discontinuities as the predominant fatigue failure mode to be addressed. The proposed Code Case N-47 fatigue strength reduction factor described in this paper is intended to do that.

The first of the two sections in the main body of this paper summarizes the proposed fatigue strength reduction factor and the experimental data and logic on which it is based. An extensive body of elevated-temperature fatigue data on weldments in austenitic stainless steels and, to a lesser extent, ferritic steels has been generated in recent years in the United States, Europe, and Japan in connection with liquid-metal fast breeder reactor development programs. Although much of these data have not been published and are available only on a restricted or foreign exchange basis, the scope of the data and the trends that they show are presented. Some open-literature papers that typify the findings are referenced and discussed.

These data, taken as a group, support the premise that metallurgical discontinuities are the principal contributor to reduced fatigue life in high-quality, ground flush, weldments. Differences in both initial and cyclic yield strengths across a weldment (weld metal, fusion line, heat-affected zone, and base metal) result in higher than nominal strains being concentrated in one or the other of the weldment constituent regions. This resulting high strain range leads to early fatigue failure in that particular constituent. The fatigue strength reduction factor is intended to address this reduced fatigue life in an easily applied design rule.

The second section of the main body of the paper describes the fatigue tests of tubular weldments conducted at ORNL to provide further support to the bases for the reduction factor. In addition to control tests on all-

base-metal tubes, axial-cycled low-cycle fatigue tests were performed on two different sets of welded tubes: (1) tubes with axial welds, and (2) tubes with circumferential welds. In the first case, the axial strain range was imposed equally on each constituent region of the weldment, and, as expected, the fatigue life of these tubes was essentially the same as that of the all-base-metal tubes. In the second case – that of the tubes with circumferential welds – the differing yield strengths produced strain concentrations that resulted in significantly reduced fatigue lives. These tubular results are presented and discussed.

BACKGROUND AND PROPOSED FATIGUE STRENGTH REDUCTION FACTOR

The number of material and process variables that influence the properties of weldments can seem bewildering and has often thwarted the development of property-specific weldment design criteria. The filler and base metal compositions, joint design, welding process and parameters, and heat treatment and aging can all affect properties. It would thus seem that a weldment fatigue assessment approach based on weldment properties would be difficult to develop. Surprisingly, a fairly consistent story emerges when the available elevated-temperature weldment fatigue data, which are from a variety of sources and for a broad range of material and process variables, are studied.

Elevated-temperature fatigue data for both austenitic stainless steel (types 304 and 316) and ferritic steel (2-1/4 Cr–1 Mo and modified 9 Cr–1 Mo) weldments have been generated, both under the U.S. Department of Energy reactor programs and under similar programs in Europe and Japan. The U.S. data appear mainly in unpublished restricted distribution reports. The foreign data are in similarly restricted reports obtained under the Department of Energy's foreign exchange agreements. In all, 15 sources of data were studied. Data for 304 stainless steel weldments are available to 593°C (1100°F); 304 and 308 (with and without controlled residual elements) were used as filler metals; and several weld processes, heat treatments, and base metal product forms were employed. For 316 stainless steel weldments, data to 625°C (1157°F) are available with 16-8-2 and 316 filler metals, and, again, a number of different variables were used in preparing the weldments. Normalized and tempered 2-1/4 Cr–1 Mo steel weldment data are available at 482°C (900°F), and modified 9 Cr–1 Mo steel data are available to 593°C (1100°F). References (7-10) typify these available data.

Weldment fatigue data are generally generated using three different types of uniaxial solid-bar specimens, as shown in Fig. 1. The first is a parallel, or longitudinal, all-weld-metal specimen; the second is a transverse all-weld-metal specimen, and the third is a transverse specimen containing both weld and base metal. This latter specimen will be referred to here as a "weldment" specimen.

The general trend of the data studied is depicted schematically in Fig. 2. Longitudinal weld metal fatigue data differ, if at all, only very slightly from fatigue data for the corresponding unaffected base metal. Weldment and transverse weld metal data, on the other hand, drop below the base metal fatigue curve in the mid-cycle region (see Refs. 8 and 9). In terms of strain range the reduction factor varies generally between 1.5 and 1.8, although, depending on weld process, the factor can be somewhat larger for 2-1/4 Cr–1 Mo steel weldments. Although the data at high and low strain ranges are sparse, it appears, as depicted in Fig. 2, that at large strain ranges the weldment data approach the base metal data. Likewise, although high-cycle-fatigue is very dependent on grain size, there is usually little difference between weldment and base metal data at very low strain ranges.

The premise is that these observed differences are largely due to the metallurgical notch effect resulting from widely varying yield strengths in weld and base metal. For both austenitic and ferritic steels the initial weld metal yield strength is usually substantially higher than that of the base metal. Although the ratio of the two decreases with temperature, weld metal yield in the temperature-range being considered here is usually about twice that of the corresponding base metal. As strain cycling occurs in a cyclic stress-strain or fatigue test, weld and base metals harden/soften depending on strain range and temperature. Although the weld metal may initially cyclically harden, it generally softens later to the point that its cyclic yield strength becomes fairly close to, or even less than, that of the base metal. Reference (9), for example, presents data for 304/308 weldments showing that at 593°C (1100°F) the base metal yield is higher than that of the weld metal during most of the life of a fatigue test, whereas the opposite is true at room temperature. In Ref. (11), 316/16-8-2 weldment fatigue specimens were instrumented with strain gages and fatigue tested at room temperature. In this case the weld metal cyclic yield strength remained higher than that of the base metal. Therefore the base metal took

a disproportionately large share of the applied strain range (recall that a "weldment" specimen contains both weld metal and base metal). As would be expected, therefore, the fatigue failure occurred in the base metal, and when the measured base metal strain ranges were used, the results correlated well with the base metal fatigue curve.

Returning to the schematic representation in Fig. 2, it is believed that at low strain ranges (high-cycle fatigue), little yielding occurs, so that the metallurgical notch effect is minimal. At large strain ranges, which are outside the normal design region, any hardening and softening occurs quickly. During most of the life of a weldment fatigue specimen the weld and base metal yield strengths are close, so that, again, the metallurgical notch effect is minimal. In summary, it is believed that the behavioral trends illustrated in Fig. 2 are explained by the yield strength variations. Anytime there is a difference in yield strength across a weldment specimen, the fatigue life will be reduced.

Now, how can this information be transformed into an elevated-temperature weldment fatigue design factor? Clearly, the case of a small weldment specimen, where a fixed cyclic strain range is imposed across a gage length that is approximately half weld and half base metal, is an extreme situation. In a real structure a reduction factor of 1.5 to 1.8, as was illustrated in Fig. 2, on strain range would generally be overly conservative. However, when welds are placed in a deformation-controlled discontinuity region of a structure, a somewhat similar, though less extreme, situation does exist, as illustrated in Fig. 3. Here, for example, a step change in the wall thickness of a pressurized vessel or pipe with a weld would result in the imposition of a relatively fixed cyclic strain range in the general vicinity of the weld.

When the ASME Code Subgroup on Elevated Temperature Design considered the available data, as described above, and the possible structural ramifications, as illustrated in Fig. 3, it was judged that a reduced factor of 1.2 on strain range would be appropriate for elevated-temperature design. In the mid-cycle range of the Code Case N-47 design fatigue curves, this corresponds approximately to a reduction factor of two on cyclic life. The actual proposed rule thus reads:

> In the vicinity of a weld (defined by ±3 × thickness to either side of the weld centerline) the fatigue evaluation shall utilize

reduced values of the allowable number of design cycles, N_d. The N_d value shall be one-half of the value permitted for the parent material.

Note that by putting the factor on cycles rather than strain range, little penalty is imposed in the high-cycle region.

CONFIRMATORY WELDED TUBE TESTS

All of the previously described fatigue tests on 316 stainless steel and 316/16-8-2 weldments were conducted on 6.35 mm (1/4 in.) diameter or smaller solid bar specimens. It was felt that a more prototypic tubular weldment specimen should be tested to gain additional confidence in the design factor proposed by the Code's Subgroup on Elevated Temperature Design.

Materials and Specimens

Specimens used in this investigation were obtained from U.S. reference heat 8092297 of type 316 stainless steel. Two different product forms of that heat were used to make specimens: (1) 50.8-mm (2-in.) flat plate for longitudinally welded specimens and (2) 50.8-mm (2-in.) round bar for circumferentially welded specimens. Specimens were prepared by first cutting grooves in the 316 stainless steel base material, as shown in Fig. 4, and then annealing the blanks at 1065°C (1950°F) for 2 hours in an argon atmosphere. The furnace was then allowed to cool to 600°C (1110°F) before removing the blanks and allowing them to cool in air to room temperature. The grooves in the blanks were then filled by cold wire gas tungsten arc welding using 1.59-mm (1/16-in.) ARCOS lot AR3018R 16-8-2 filler wire. Tubular specimens were machined from these blanks such that the axis of the specimens was in the rolled direction of the plate or axis of the bar. Circumferentially welded specimens were machined such that the 6.35-mm (0.25-in.) weld was located in the center of the gage area (Fig. 4). All specimens were tested in their as-welded state.

Apparatus and Test Procedure

All of the tests were conducted on MTS closed-loop hydraulic test equipment in static laboratory air at 550°C (1022°F) and at a strain rate, $\dot{\varepsilon}$, of 0.001 s^{-1}. Strain was applied using a fully reversed low-cycle fatigue ramp function to yield a strain range, $\Delta\varepsilon$. Four strain ranges were

chosen for this study, 1.5, 1.0, 0.6, and 0.4%. In order to determine if the tubular specimen geometry would yield significantly different results than the solid bar data, a series of 316 stainless steel base metal specimens was prepared from 50.8-mm (2-in.) round bar and tested to establish a base line. Longitudinal and circumferential, or transverse, weldment specimens were then tested at each of the four strain ranges. All of the tests were done in axial strain control using an MTS 25.4-mm (1-in.) gage length high-temperature extensometer. An RF generator was used with a series of three induction coils around each specimen to establish the desired temperature profile. Because of the problem of trying to fail a specimen in the control gage length and not at some geometric discontinuity, a slight temperature gradient was established inside the gage length. The temperature at the center of the gage length was at 550°C (1022°F), but a gradient of 10°C (18°F) was established to the edge of the gage length. This resulted in the gage length temperature being 540°C (1004°F) at the edges and 550°C (1022°F) at the center, about a 2% variation in temperature. All specimens were tested to failure, which was taken as a 50% reduction in the applied load from the strain hardened state.

In addition to the above mentioned tests, two additional tests were conducted to determine the strain distribution over the gage length of the circumferential weldment, both at room temperature and at elevated temperature. For the room-temperature test the specimen was instrumented with eight 1.59-mm (1/16-in.) foil gages and a 25.4-mm (1-in.) MTS extensometer for control (Fig. 5). The high-temperature test specimen was instrumented with two 25.4-mm (1-in.) MTS extensometers with one of them fitted with offset probes to measure only the strain in the weld. After the modified extensometer was fitted to the specimen an in-place room-temperature calibration was done on the specimen in its elastic range to 250 microstrain. Both strain distribution tests were conducted at a nominal controlled strain range of 0.6%.

Strain Distribution Test Results

Results of both the room-temperature and high-temperature strain distribution tests can be seen in Fig. 6. Note that in looking at the room-temperature data, the 316 stainless steel base metal experiences a higher strain state during the entire test, with the specimen failing just inside the gage length in the base metal. A hardness profile done on

an untested specimen, Fig. 7, shows that the weld metal is harder than the base metal at room temperature. This is in good agreement with Ref. (11) and the strain distribution test; both imply the weld metal has a higher yield strength than the base metal. On the other hand, the elevated-temperature strain distribution test shows that the 16-8-2 weld metal experienced a higher strain state during most of the test, with that specimen failing at the center of the weld. Miner's rule, $\Sigma\ N/N_f = D = 1$, was applied to the elevated-temperature strain distribution test data using a fatigue curve obtained from Idaho National Engineering Laboratory data on transverse weld metal; it was found that D was equal to 0.98 when the first visible crack appeared. This result implies that the weld metal had accumulated sufficient damage to fail, and indeed the failure occurred in the weld. Care was taken during this test to maintain as closely as possible a uniform temperature across the total gage length so as not to bias the test results.

Fatigue Test Results

Several 316 stainless steel base metal specimens were tested in order to compare their results with the solid bar data and also to establish a base metal curve for the tubular specimen geometry. Figure 8 shows that at high strain ranges the sets of data are nearly identical, but at lower strain ranges the solid bar data show longer life than the tubular fatigue specimens. It should be noted that failure was taken as complete fracture for the solid bar specimens vs a 50% reduction in the strain-hardened load for the tubular specimens. Similar work done at Oak Ridge National Laboratory on 316 stainless steel at strain ranges even higher than those used here showed the tubular specimens to have longer lives.

Longitudinal and circumferential weldment specimens were then tested and compared to the 316 stainless steel tubular base line curve. Figure 9 shows the 316 stainless steel base metal curve and both longitudinal and circumferential weldment data points. As expected, the longitudinal weldment data fall very nearly on the base metal curve, since all of the weldment sees the same axial strain range, but the circumferential weldment data fall below the base line curve. The solid bar specimen tests described earlier showed a 1.5 to 1.8 reduction in strain range from base metal to weldments. Likewise, these data show a reduction of 1.5 on strain range from the base metal to circumferential weldment. Also shown in Fig. 9 is a

plot of the Code Case N-47 316 stainless steel design curve for the temperature range 538 to 699°C (1000 to 1200°F) and the Code curve with the proposed weldment design factor applied.

From Fig. 9 it becomes obvious that the weldment data use up much of the safety factor of 2 on strain range or 20 on cycles put in the Code to cover factors affecting life other than the presence of a weld. These factors include such considerations as surface finish, size effects, material variability, environmental considerations, and residual stresses due to fabrication (except for welds). If the safety factor of 20 on cycles to failure were applied to the circumferential weldment data it would be found that these "design" points would fall slightly below the proposed weldment design curve for fatigue. But, as was stated earlier in this paper, welds are not usually put in regions of very high strain concentration nor do welds normally compose 1/4 to 1/3 of a region experiencing a fixed cyclic deformation such as our test specimen experienced. This goes back to the explanation as to why a factor of 1.2 reduction in strain range was used to arrive at the proposed design curve instead of the experimentally determined factor of 1.5 to 1.8. Thus, it is believed that the data generated thus far support the need for, and suitability of, the proposed Code factor for the fatigue of welded joints at elevated temperature.

Summary and Conclusions

The objective of this study was to determine the suitability of the fatigue design factor proposed by the Subgroup on Elevated Temperature Design for Weldments. A review of fatigue data available at elevated temperatures on weldment materials used in nuclear components was carried out. These data were generated from solid bar specimens, and it was determined from them that a reduction factor of two on the number of design cycles for a given strain range relative to the design base metal curve would be an effective design approach for welded joints. A series of more prototypic tubular weldment specimens were then tested to gain additional confidence in the proposed Code factor. Results of these tests fell slightly below data generated from the solid bar tests. An argument based on the premise that in-service welded joints would not experience as severe a strain condition as a test specimen was made and applied to both solid bar and tubular weldment data. Based on this information it was concluded that the factor of two on design cycles was appropriate. An effort is now under

way to conduct fully reversed torsional fatigue tests on 316/16-8-2 tubular weldment specimens. An investigation into this mode of failure will help to better understand how weldments differ from base metal in fatigue characteristics and will add to the bases used in determining the need for a weldment design reduction factor.

ACKNOWLEDGMENTS

The authors wish to thank T. G. Hill for his support in instrumenting and conducting the tubular fatigue tests and also D. T. Godwin for his support in plotting the data and preparing the figures for this paper.

REFERENCES

1. Case N-47-22, Class 1 Components in Elevated Temperature Service, Section III, Division 1, Cases of the ASME Boiler and Pressure Vessel Code, April 1984.

2. The Phenix Nuclear Plant After Three Years of Operation, Centrale Phenix, July 14, 1977.

3. F. Conte, M. Sauvage, and J.-F. Roumailhac, "The Intermediate Heat Exchanger Leak on Phenix Plant and Their Repair," pp. 291-296 in Optimization of Sodium-Cooled Fast Reactors, British Nuclear Energy Society, London, 1978.

4. R. R. Matthews and K. J. Henry, "Location and Repair of the DFR Leak," Nuclear Engineering, Vol. 13, No. 149, pp. 840-844 (October 1968).

5. U. S. Nuclear Regulatory Commission, Safety Evaluation Report Related to the Construction of the Clinch River Breeder Reactor Plant, NUREG-0968, Vol. 1, March 1983.

6. D. S. Griffin, "Elevated-Temperature Structural Design Evaluation Issues in LMFBR Licensing," Proceedings of Eighth International Conference on Structural Mechanics in Reactor Technology, Vol. L, Paper L9/1, Brussels, August 1985.

7. S. Usami, Y. Fukuda, and S. Shida, "Microcrack Initiation, Propagation, and Threshold in Elevated Temperature Inelastic Fatigue," Preprint 83-PVP-97, The American Society of Mechanical Engineers, 1983.

8. G. E. Korth and M. D. Harper, "Fatigue and Creep-Fatigue Behavior of Irradiated and Unirradiated Type 308 Stainless Steel Weld Metal at Elevated Temperatures," pp. 172-190 in Properties of Reactor Structural Alloys after Neutron or Particle Irradiation: A Symposium, Philadelphia, American Society for Testing and Materials STP-570, 1976.

9. C. R. Brinkman, G. E. Korth, and J. M. Beeston, "Comparison of the Strain-Controlled Low Cycle Fatigue Behavior of Stainless Type 304/308 Weld and Base Material," Proceedings of International Conference on Creep and Fatigue in Elevated Temperature Applications, Institution of Mechanical Engineers, 1973.

10. R. W. Swindeman and B. C. Williams, "Fatigue of Bainitic 2 1/4 Cr-1 Mo Steel Weldments at 482°C," Preprint 84-PVP-57, The American Society of Mechanical Engineers, 1984.

11. G. E. Korth and M. D. Harper, "Strain Distributions in a Type 316/16-8-2 Stainless Steel Weldment During Cyclic Loading," Preprint 84-PVP-26, The American Society of Mechanical Engineers, 1984 (to be published in the Journal of Pressure Vessel and Piping).

DISCLAIMER

This report was prepared as an account of work sponsored by an agency of the United States Government. Neither the United States Government nor any agency thereof, nor any of their employees, makes any warranty, express or implied, or assumes any legal liability or responsibility for the accuracy, completeness, or usefulness of any information, apparatus, product, or process disclosed, or represents that its use would not infringe privately owned rights. Reference herein to any specific commercial product, process, or service by trade name, trademark, manufacturer, or otherwise does not necessarily constitute or imply its endorsement, recommendation, or favoring by the United States Government or any agency thereof. The views and opinions of authors expressed herein do not necessarily state or reflect those of the United States Government or any agency thereof.

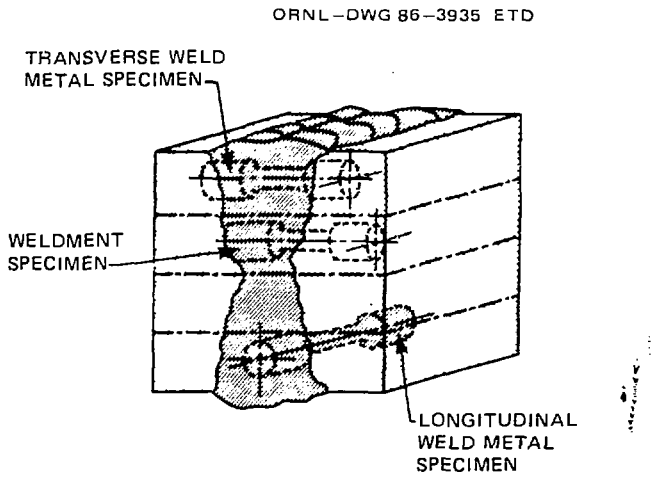

Fig. 1. Orientations of weldment fatigue test specimens.

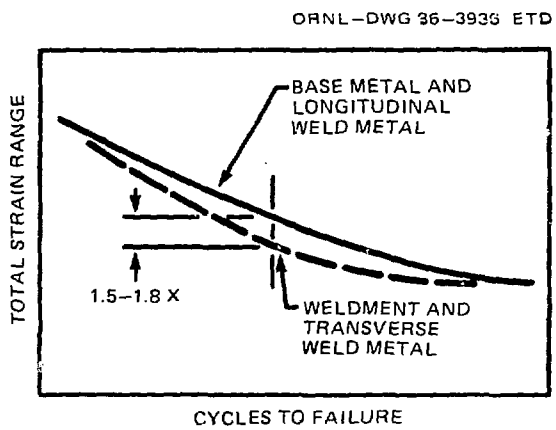

Fig. 2. Trends of available weldment fatigue data.

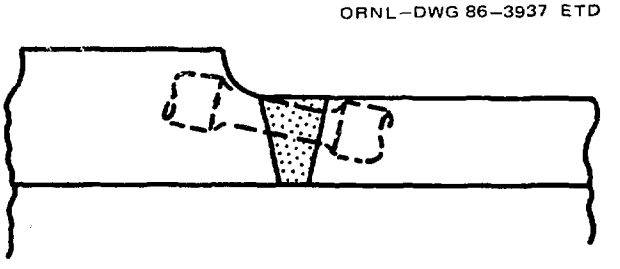

Fig. 3. Schematic of weld in a deformation-controlled discontinuity region of a structure.

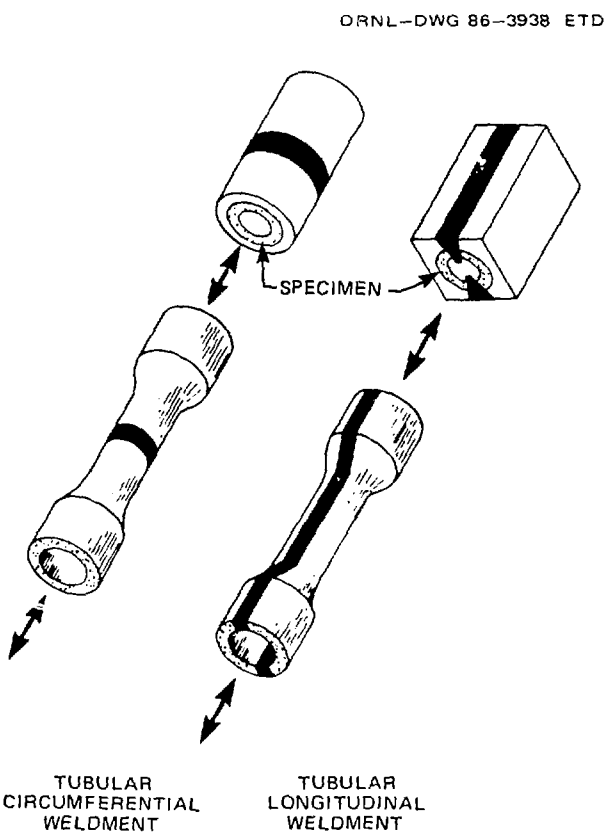

Fig. 4. Method of obtaining tubular weldment specimens.

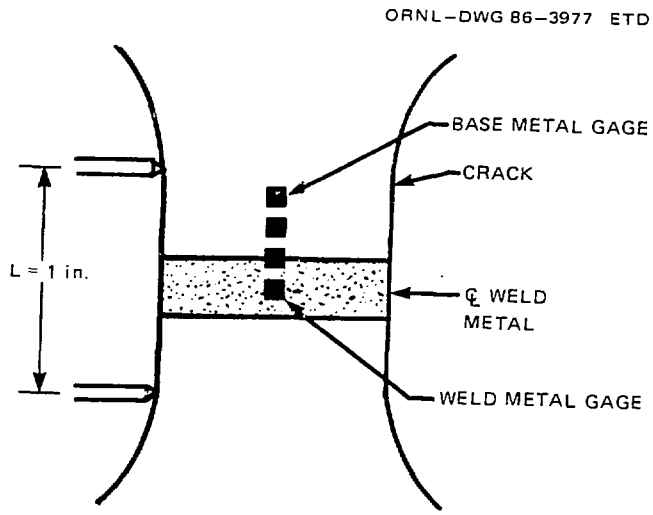

Fig. 5. Strain gage layout on room-temperature test specimen.

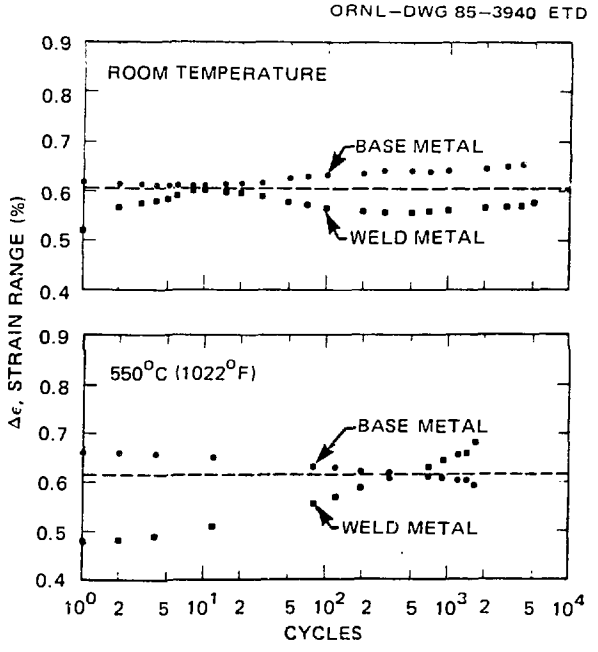

Fig. 6. Measured strain ranges in weld and base metals for room- and elevated-temperature tests.

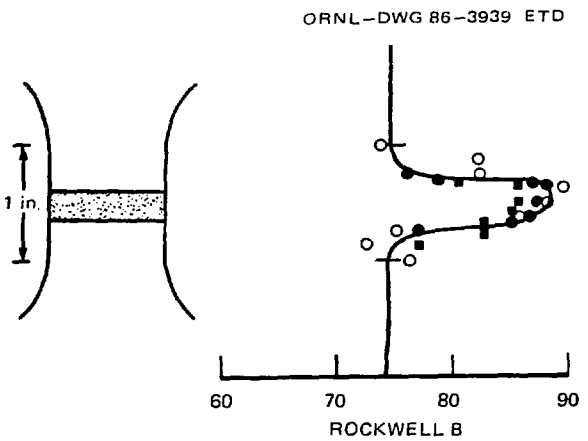

Fig. 7. Hardness profile across tubular weldment specimen. The various data symbols represent separate axial scans around the specimen.

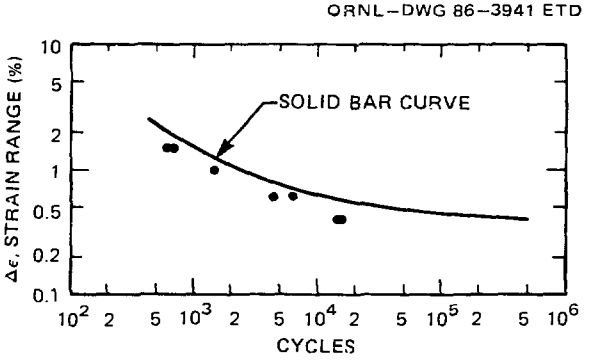

Fig. 8. Comparison of base metal fatigue data for tubular data with solid bar data.

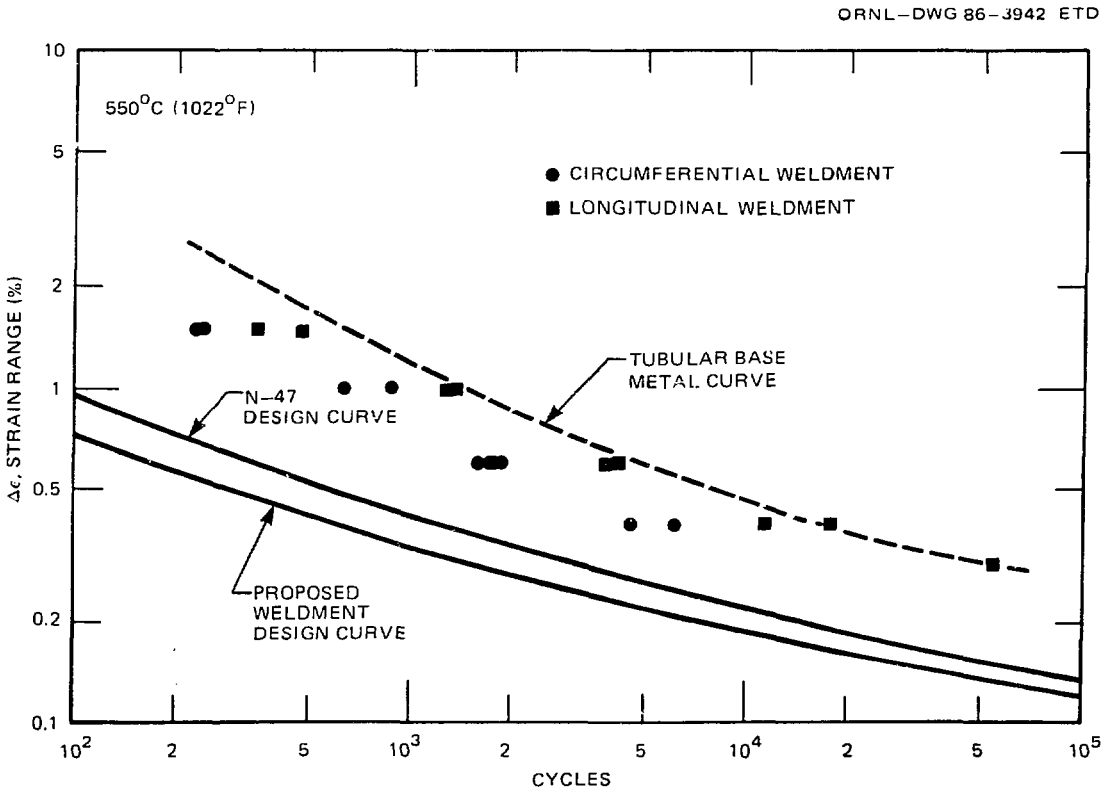

Fig. 9. Comparison of tubular weldment fatigue data with tubular base metal data.